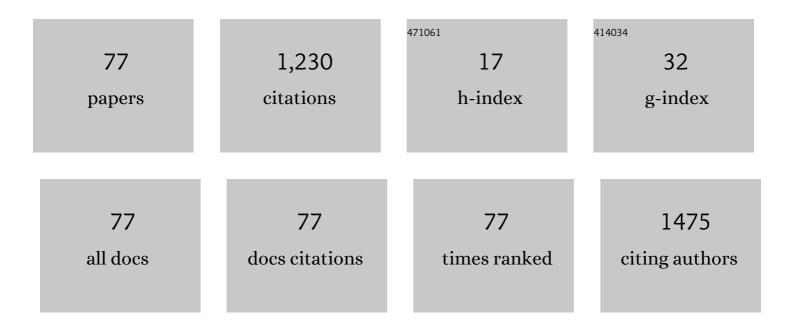
## Jianhong Yang

List of Publications by Year in descending order

Source: https://exaly.com/author-pdf/7595779/publications.pdf Version: 2024-02-01



#	Article	IF	CITATIONS
1	Investigation of resistive switching in Cu-doped HfO <sub>2</sub> thin film for multilevel non-volatile memory applications. Nanotechnology, 2010, 21, 045202.	1.3	262
2	Strong Dzyaloshinskii-Moriya Interaction and Origin of Ferroelectricity in <mml:math xmlns:mml="http://www.w3.org/1998/Math/MathML" display="inline"&gt;<mml:msub><mml:mi>Cu</mml:mi><mml:mn>2</mml:mn></mml:msub><mml:msub><mm Physical Review Letters, 2012, 109, 107203.</mm </mml:msub></mml:math 	l:mi>đSeO<	/mml:mi> <mm< td=""></mm<>
3	Highly Stable Radiation-Hardened Resistive-Switching Memory. IEEE Electron Device Letters, 2010, 31, 1470-1472.	2.2	69
4	Tunable Fano resonances based on microring resonator with feedback coupled waveguide. Optics Express, 2016, 24, 20187.	1.7	58
5	Mode and Polarizationâ€Division Multiplexing Based on Silicon Nitride Loaded Lithium Niobate on Insulator Platform. Laser and Photonics Reviews, 2022, 16, .	4.4	42
6	Experimental demonstration of an optical Feynman gate for reversible logic operation using silicon micro-ring resonators. Nanophotonics, 2018, 7, 333-337.	2.9	35
7	Ultra-compact dual-polarization silicon mode-order converter. Optics Letters, 2019, 44, 4179.	1.7	33
8	Dry electrode for the measurement of biopotential signals. Science China Information Sciences, 2011, 54, 2435-2442.	2.7	30
9	Improving the electrical performance of resistive switching memory using doping technology. Science Bulletin, 2012, 57, 1235-1240.	1.7	29
10	On-chip reconfigurable and scalable optical mode multiplexer/demultiplexer based on three-waveguide-coupling structure. Optics Express, 2018, 26, 22366.	1.7	29
11	PDMS-Assisted Microfiber M-Z Interferometer With a Knot Resonator for Temperature Sensing. IEEE Photonics Technology Letters, 2019, 31, 337-340.	1.3	26
12	Single-step etched grating couplers for silicon nitride loaded lithium niobate on insulator platform. APL Photonics, 2021, 6, 086108.	3.0	24
13	Strong single-ion anisotropy and anisotropic interactions of magnetic adatoms induced by topological surface states. Physical Review B, 2012, 85, .	1.1	22
14	Reconfigurable On-Chip Mode Exchange for Mode-Division Multiplexing Optical Networks. Journal of Lightwave Technology, 2019, 37, 1008-1013.	2.7	22
15	A novel Cu <inf>x</inf> Si <inf>y</inf> O resistive memory in logic technology with excellent data retention and resistance distribution for embedded applications. , 2010, , .		21
16	Band alignment of two-dimensional h-BN/MoS2 van der Waals heterojunction measured by X-ray photoelectron spectroscopy. Journal of Alloys and Compounds, 2020, 834, 155108.	2.8	20
17	Strain modulation of electronic and optical properties of monolayer MoSi2N4. Physica E: Low-Dimensional Systems and Nanostructures, 2022, 135, 114964.	1.3	20
18	Experimental demonstration of a reconfigurable electro-optic directed logic circuit using cascaded carrier-injection micro-ring resonators. Scientific Reports, 2017, 7, 6410.	1.6	18

#	Article	IF	CITATIONS
19	Integrated Subwavelength Gratings on a Lithium Niobate on Insulator Platform for Mode and Polarization Manipulation. Laser and Photonics Reviews, 2022, 16, .	4.4	16
20	Independently tunable double Fano resonances based on waveguide-coupled cavities. Optics Letters, 2019, 44, 3154.	1.7	15
21	Reconfigurable Electro-optic Logic Circuits Using Microring Resonator-Based Optical Switch Array. IEEE Photonics Journal, 2016, 8, 1-8.	1.0	14
22	Tuning the mechanical and electronic properties and carrier mobility of phosphorene <i>via</i> family atom doping: a first-principles study. Journal of Materials Chemistry C, 2020, 8, 14902-14909.	2.7	14
23	A Gradient-Oriented Binary Search Method for Photonic Device Design. Journal of Lightwave Technology, 2021, 39, 2407-2412.	2.7	14
24	On-chip switchable and reconfigurable optical mode exchange device using cascaded three-waveguide-coupling switches. Optics Express, 2020, 28, 9552.	1.7	13
25	Electro-optic directed XOR logic circuits based on parallel-cascaded micro-ring resonators. Optics Express, 2015, 23, 26342.	1.7	12
26	Graphene-assisted all-optical tunable Mach–Zehnder interferometer based on microfiber. Optics Communications, 2018, 428, 77-83.	1.0	12
27	Ultra-compact reflective mode converter based on a silicon subwavelength structure. Applied Optics, 2020, 59, 2754.	0.9	12
28	Tunable Fano resonance in mutually coupled micro-ring resonators. Applied Physics Letters, 2017, 111, .	1.5	11
29	On-chip optical parity checker using silicon photonic integrated circuits. Nanophotonics, 2018, 7, 1939-1948.	2.9	11
30	Broadband Nonvolatile Tunable Mode-Order Converter Based on Silicon and Optical Phase Change Materials Hybrid Meta-Structure. Journal of Lightwave Technology, 2020, 38, 1874-1879.	2.7	11
31	Ultra-compact switchable mode converter based on silicon and optical phase change material hybrid metastructure. Optics Communications, 2020, 473, 125889.	1.0	11
32	Experimental realization of an optical digital comparator using silicon microring resonators. Nanophotonics, 2018, 7, 669-675.	2.9	10
33	Multi-Channel Parallel Silicon Mode-Order Converter for Multimode On-Chip Optical Switching. IEEE Journal of Selected Topics in Quantum Electronics, 2020, 26, 1-6.	1.9	10
34	High sensitivity temperature sensor based on a PDMS-assisted bow-shaped fiber structure. Optics Communications, 2021, 481, 126536.	1.0	10
35	Analysis of dark current dependent upon threading dislocations in Ge/Si heterojunction photodetectors. Microelectronics International, 2012, 29, 136-140.	0.4	9
36	Experimental realization of a CMOS-compatible optical directed priority encoder using cascaded micro-ring resonators. Nanophotonics, 2018, 7, 727-733.	2.9	8

#	Article	IF	CITATIONS
37	Determination of band alignment in two-dimensional h-BN/WS2 van der waals heterojunction by X-ray photoelectron spectroscopy. Journal of Alloys and Compounds, 2021, 854, 157301.	2.8	8
38	A novel buried-gate static induction transistor with diffused source region. Semiconductor Science and Technology, 2004, 19, 152-156.	1.0	7
39	Simulation and Demonstration of Directed XOR/XNOR Logic Gates Using Two Cascaded Microring Resonators. IEEE Photonics Journal, 2016, 8, 1-11.	1.0	7
40	Mode-Oriented Permutation Cipher Encryption and Passive Signal Switching Based on Multiobjective Optimized Silicon Subwavelength Metastructures. ACS Photonics, 2020, 7, 2163-2172.	3.2	7
41	Influence of AlGaN back-barrier on irradiation tolerance of AlGaN/AlN/GaN HEMTs. Physics Letters, Section A: General, Atomic and Solid State Physics, 2021, 410, 127527.	0.9	7
42	Ge-on-insulator wafer with ultralow defect density fabricated by direct condensation of SiGe-on-insulator structure. Applied Surface Science, 2015, 356, 1052-1057.	3.1	6
43	Demonstration of an optical directed half-subtracter using integrated silicon photonic circuits. Applied Optics, 2018, 57, 2564.	0.9	6
44	Dipole-regulated bandgap and high electron mobility for bilayer Janus MoSiGeN4. Applied Physics Letters, 2022, 120, .	1.5	6
45	An Improved Helical Resonator Design for Rubidium Atomic Frequency Standards. IEEE Transactions on Instrumentation and Measurement, 2010, 59, 1678-1685.	2.4	5
46	High sensitivity biosensors based on germanium nanowires fabricated by Ge condensation technique. Materials Letters, 2016, 172, 142-145.	1.3	5
47	Properties of monolayer black phosphorus affected by uniaxial strain. Physica E: Low-Dimensional Systems and Nanostructures, 2020, 117, 113834.	1.3	5
48	Valence band offset of ReS2/BN heterojunction measured by X-ray photoelectron spectroscopy. Physics Letters, Section A: General, Atomic and Solid State Physics, 2021, 392, 127142.	0.9	5
49	Ultraviolet-electrical erasing response characteristics of Ag@SiO2 core-shell functional floating gate organic memory. Organic Electronics, 2021, 93, 106149.	1.4	5
50	Two-dimensional electron gas (2DEG) mobility affected by the in mole fraction fluctuation in In x Al 1â^'x N/GaN heterostructures. Physica E: Low-Dimensional Systems and Nanostructures, 2016, 83, 207-210.	1.3	4
51	A theory study of the multiplication characteristics of InP/InGaAs avalanche photodiodes with double multiplication layers and double charge layers. Optics Communications, 2016, 374, 114-118.	1.0	4
52	Modeling a novel InP/InGaAs avalanche photodiode structure: Reducing the excess noise factor. Optics Communications, 2019, 435, 374-377.	1.0	4
53	Integrated non-blocking optical router harnessing wavelength- and mode-selective property for photonic networks-on-chip. Optics Express, 2021, 29, 1251.	1.7	4
54	Demonstration of various optical directed logic operations by using an integrated photonic circuit. Optics Letters, 2021, 46, 2457.	1.7	4

#	Article	IF	CITATIONS
55	On-Chip Non-Blocking Optical Mode Exchanger for Mode-Division Multiplexing Interconnection Networks. Journal of Lightwave Technology, 2021, 39, 6563-6571.	2.7	4
56	All-Optical Tunable Whispering Gallery Modes in a Polymer Bottle Micro-Resonator. IEEE Photonics Technology Letters, 2021, 33, 97-100.	1.3	4
57	Study on Effects of Different Metallic Vane-Loaded Helix Slow-Wave Structures in Traveling-Wave Tubes. Journal of Infrared, Millimeter, and Terahertz Waves, 2009, 30, 611-621.	1.2	3
58	The design and implementation of wireless temperature and humidity control system based on nRF905. , 2015, , .		3
59	Demonstration of a Silicon Photonic Circuit for Half-Add Operations Using Cascaded Microring Resonators. IEEE Photonics Journal, 2017, 9, 1-9.	1.0	3
60	Organic Field-Effect Transistor Memory Device Based on an Integrated Carbon Quantum Dots/Polyvinyl Pyrrolidone Hybrid Nanolayer. Electronics (Switzerland), 2020, 9, 753.	1.8	3
61	On-chip scalable mode-selective converter based on asymmetrical micro-racetrack resonators. Nanophotonics, 2020, 9, 1447-1455.	2.9	3
62	Analysis of Improved 2D Electron Gas Mobility in InAlN/AlN/InGaN Highâ€Electronâ€Mobility Transistors with GaN Interlayer. Physica Status Solidi - Rapid Research Letters, 2022, 16, .	1.2	3
63	The same band alignment of two hybrid 2D/3D vertical heterojunctions formed by combining monolayer MoS2 with semi-polar (11–22) GaN and c-plane (0001) GaN. Applied Surface Science, 2022, 599, 153965.	3.1	3
64	An analytical model for the saturation characteristics of bipolar-mode static induction transistors. Solid-State Electronics, 1999, 43, 823-827.	0.8	2
65	Demonstration of a Microfiber-Based Add–Drop Filter Using One Tapered Fiber. IEEE Photonics Journal, 2018, 10, 1-6.	1.0	2
66	Potential barrier height dependence on biased voltages of static induction thyristors. , 2012, , .		1
67	Theoretical studies of the capacitanceâ€voltage characteristics of metalâ€ferroelectricâ€ <scp>GaN</scp> structures. International Journal of Numerical Modelling: Electronic Networks, Devices and Fields, 2012, 25, 96-101.	1.2	1
68	Ultra-Compact Sb <sub>2</sub> S <sub>3</sub> -Silicon Hybrid Integrated Arbitrarily Cascaded Tunable Mode Converter. IEEE Photonics Journal, 2022, 14, 1-7. Mode Converter. IEEE Photonics Journal, 2022, 14, 1-7.	1.0	1
69	altimg="si7.svg"> <mml:mrow><mml:mi mathvariant="normal">144</mml:mi><mml:mi mathvariant="normal"&gt;m</mml:mi </mml:mrow> Ultra-broadband polarization beam splitter with tunable transmissions based on silicon-Ge <mml:math xmlns:mml="http://www.w3.org/1998/Math/MathML" display="inline" id="d1e388"</mml:math 	1.0	1
70	elting="si0.svg"> summing by summing weather the structure under the high-level injection condition. Semiconductor Science and Technology, 2003, 18, L31-L34.	1.0	0
71	Design and numerical simulation of a humidity sensor based on CMOS fabrication technology. Physics Procedia, 2011, 18, 31-39.	1.2	0
72	Transfer characteristics in a GaN MFSFET: comparison with a conventional GaN MOSFET. International Journal of Electronics, 2012, 99, 987-993.	0.9	0

#	Article	IF	CITATIONS
73	Controllable decay in an optical waveguide system. AIP Advances, 2016, 6, 095212.	0.6	0
74	p-n junction theory in view of excess majority carriers. Europhysics Letters, 2017, 120, 28004.	0.7	0
75	On-chip Reconfigurable Mode Converter Compatible with WDM Using Parallel Micro-ring Resonators. , 2019, , .		Ο
76	Theoretical Study on InAlAs/InGaAs Singleâ€Photon Avalanche Detectors with Selfâ€Feedback. Physica Status Solidi (A) Applications and Materials Science, 2020, 217, 2000053.	0.8	0
77	Analytical model for the potential barrier height in depleted channel formed by P-N junctions. Chinese Science Bulletin, 2017, 62, 3392-3399.	0.4	0